Higgs boson production via the Bjorken process $e^+e^- \to H^0\mu^+\mu^-$ at high energy e^+e^- colliders

C.-M. J. Chen, Jiunn-Wei Chen, and W-Y. P. Hwang
Department of Physics, National Taiwan University, Taipei, Taiwan 10764, Republic of China
(Received 13 January 1994)

Production of the standard Higgs boson via the Bjorken process, $e^+e^- \to H^0\mu^+\mu^-$, at the center-of-mass energy $\sqrt{s} \approx 200$ GeV (i.e., for the CERN Large Electron-Positron Collider LEP II) is investigated in detail for a Higgs boson mass ranging from 60 GeV to about 120 GeV. We focus on physical quantities which have not been emphasized so far, including the differential cross sections in the various μ^+ (or μ^-) scattering angles (with the remaining angles integrated out completely) and the anticipated charge asymmetry. Numerical results on these quantities, in addition to the total production cross section, are described.
PACS number(s): 14.80.Bn, 13.10.+q

I. INTRODUCTION

In recent years, the search for the Higgs particle has become one of the most important issues related to the Glashow-Salam-Weinberg (GSW) electroweak theory [1], which is now christened as "the standard model" in view of its amazing successes [2] in accounting for the phenomenology at currently accessible energies. Consistency arguments [3], together with results of numerous Higgs particle searches [4], give a lower bound of 48 GeV and an upper bound of about 1 TeV for the mass of the standard model Higgs particle.

There are processes which may be used to search for the Higgs particle. Wilczek [5] suggested to look for the Higgs particle in the decay of quarkonium vector-meson states $(Q\bar{Q}) \to H+\gamma$. Cahn, Chanowitz, and Fleishon [6] considered the Z^0 decay, $Z^0 \to H + \gamma$. It is clear that, although the monochromatic photon produced in these decays provides a clean signature, the branching ratios are rather small and the range of the Higgs particle mass being searched is limited by the vector-meson mass. Ellis, Gaillard, and Nanopoulos [7], and subsequently many others [8–10], have considered the associated production $e^+e^- \to Z^0H$, which is useful for high-energy e^+e^- colliders. Such associated production of the standard model Higgs boson may be very useful for the next generation of e^+e^- colliders (say with $\sqrt{s}$ not less than energies of the CERN Large Electron-Positron Collider LEP II, which is around 200 GeV). Another unique process to search for the Higgs boson is $e^+e^- \to H^0l^+l^-$ which is usually referred to as the Bjorken process [11] and has in fact been used by the experiments conducted at LEP I. Recently, Glashow and Jenkins [12] have considered the total cross section for the Bjorken process while Terazawa and Biyajima [13] have studied the invariant-mass and collinearity-angle distributions for the Bjorken process and addressed the question associated with the background process $e^+e^- \to f\bar{f} \to f'l^+\nu_l + \bar{f}'l^-\bar{\nu}_l$. (Here the collinearity angle refers to the angle θ_c between l^+ and l^-. The collinearity-angle distribution is just the differential cross section in $\cos\theta_c$ with the remaining variables integrated out completely.)

The primary objective of this work, which is a relatively straightforward one, is to investigate whether the Bjorken process would continue to be useful for experimental searches of the standard Higgs boson at LEP II energies, i.e., at a center-of-mass energy $\sqrt{s}$ of around 200 GeV. The high-mass range for the Higgs boson mass considered in the present investigation is chosen in view of the latest experimental situation [4] and, of course, it gives rise to results somewhat orthogonal to previous studies [12,13]. Furthermore, our primary focus is on those physical quantities which may eventually become of experimental interest but have not been emphasized so far by previous authors [12,13], including the differential cross sections in the various μ^+ (or μ^-) scattering angles (with the remaining angles integrated out completely) and the anticipated charge asymmetry. These observables will be of practical use when a sufficient number of "Higgs-like" particles have been observed experimentally, since then there is a need to determine if the couplings of the "Higgs particle" to other particles are exactly those given by GSW electroweak theory. Numerical results on these observables, in addition to the total production cross section, are described in the next section. It is clear that the emphasis in this paper is complementary to those studied previously by Glashow and Jenkins [12], who calculated only the total cross section, and by Terazawa and Biyajima [13], who investigated the observables which require simultaneous precision measurements of both μ^+ and μ^-.

II. FORMULATION AND NUMERICAL RESULTS

Among the possible Bjorken processes $e^+e^- \to H^0l^+l^-$, it is of particular interest to consider the case that the flavor of the final leptons differs from the initial one, say, $e^+e^- \to H^0\mu^+\mu^-$. Since the coupling of the standard model Higgs particle to a particle is proportional to the mass of the particle, the Bjorken process $e^+e^- \to H\mu^+\mu^-$ is described, to a very good approximation, by the diagram in which the Higgs particle originates from the intermediate Z^0 in the well-known s-channel process $e^+e^- \to Z^{0*} \to \mu^+\mu^-$. The process is illustrated by Fig. 1(a). The corresponding T-matrix element, or the transition amplitude, is then given by

$$T_{fi} = \frac{1}{16\sqrt{2}} \frac{e^3}{\sin^3\theta_W \cos^3\theta_W} \frac{1}{M_Z^3\sqrt{E_H}} \frac{1}{1+M_Z^{-2}(p_3+p_4)^2 - iM_Z^{-1}\Gamma_Z} \frac{1}{1+M_Z^{-2}(p_1+p_2)^2 - iM_Z^{-1}\Gamma_Z}$$
$$\times[\bar{u}(p_4)\gamma_\mu(g_V^\mu + g_A^\mu\gamma_5)v(p_3)\bar{v}(p_2)\gamma_\mu(g_V^e + g_A^e\gamma_5)u(p_1)], \quad (1)$$

where p_1, p_2, p_3, and p_4 are, respectively, the four-momenta of e^-, e^+, μ^+, and μ^-. E_H is the energy of the Higgs particle, and M_Z and Γ_Z are the mass and width of the Z^0 boson. Note that the other diagram as illustrated by Fig. 1(b) gives rise to a contribution of order $O(m_\mu/M_Z)$, which is clearly negligible for the purpose of the present paper.

For the sake of illustration, we use [2] $M_Z = 91.173$ GeV and $\Gamma_Z = 2.487$ GeV. To obtain sample numerical results, we also adopt [2] $\sin^2\theta_W = 0.2325$, $e^2/4\pi = 1/128$ (a value more appropriate for energies near the Z^0 mass), $g_A^\mu = g_A^e = -1$, and $g_V^\mu = g_V^e = 4\sin^2\theta_W - 1$.

Differential cross sections for $e^+e^- \to H^0\mu^+\mu^-$ in the center-of-mass (c.m.) frame may be obtained via the standard formula

$$d\sigma = \frac{1}{2}\frac{d^3p_3}{(2\pi)^3}\frac{d^3p_4}{(2\pi)^3}\frac{d^3p_5}{(2\pi)^3}(2\pi)^4\delta^4(p_3+p_4+p_5-p_1-p_2)\bar{\sum}|T_{fi}|^2, \quad (2)$$

where p_5 is the four-momentum of the Higgs particle and $\bar{\sum}$ indicates summation over final spins as well as averaging over initial spins. The result on $\bar{\sum}|T_{fi}|^2$ is given by

$$\bar{\sum}|T_{fi}|^2 = \frac{1}{1024}\frac{e^6}{(\sin\theta_W\cos\theta_W)^6}\frac{1}{M_Z^6 E_1E_2E_3E_4E_H}$$
$$\times\frac{1}{[1+M_Z^{-2}(p_3+p_4)^2]^2 + M_Z^{-2}\Gamma_Z^2}\frac{1}{[1+M_Z^{-2}(p_1+p_2)^2]^2 + M_Z^{-2}\Gamma_Z^2}$$
$$\times\{c_1(p_4\cdot p_2 p_3\cdot p_1 + p_4\cdot p_1 p_3\cdot p_2) + c_5(p_4\cdot p_2 p_3\cdot p_1 - p_4\cdot p_1 p_3\cdot p_2)$$
$$-c_2 m_e^2 p_4\cdot p_3 - c_3 m_\mu^2 p_2\cdot p_1 + 2c_4 m_e^2 m_\mu^2\}, \quad (3)$$

where m_e and m_μ are, respectively, the electron and muon masses. The coefficients c_i are specified by

$$c_1 \equiv [(g_V^\mu)^2 + (g_A^\mu)^2][(g_V^e)^2 + (g_A^e)^2],$$
$$c_2 \equiv [(g_V^\mu)^2 + (g_A^\mu)^2][(g_V^e)^2 - (g_A^e)^2],$$
$$c_3 \equiv [(g_V^\mu)^2 - (g_A^\mu)^2][(g_V^e)^2 + (g_A^e)^2], \quad (4)$$
$$c_4 \equiv [(g_V^\mu)^2 - (g_A^\mu)^2][(g_V^e)^2 - (g_A^e)^2],$$
$$c_5 \equiv 4(g_V^\mu)(g_A^\mu)(g_V^e)(g_A^e).$$

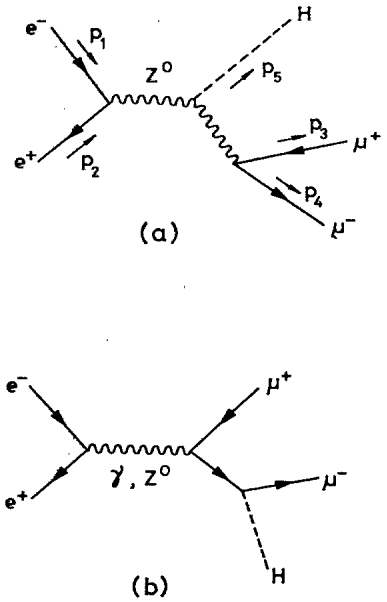

FIG. 1. Diagrams for the Bjorken process $e^+e^- \to H^0\mu^+\mu^-$: (a) the dominant contribution and (b) the contributions of order $O(m_\mu/M_Z)$ compared to the leading diagram.

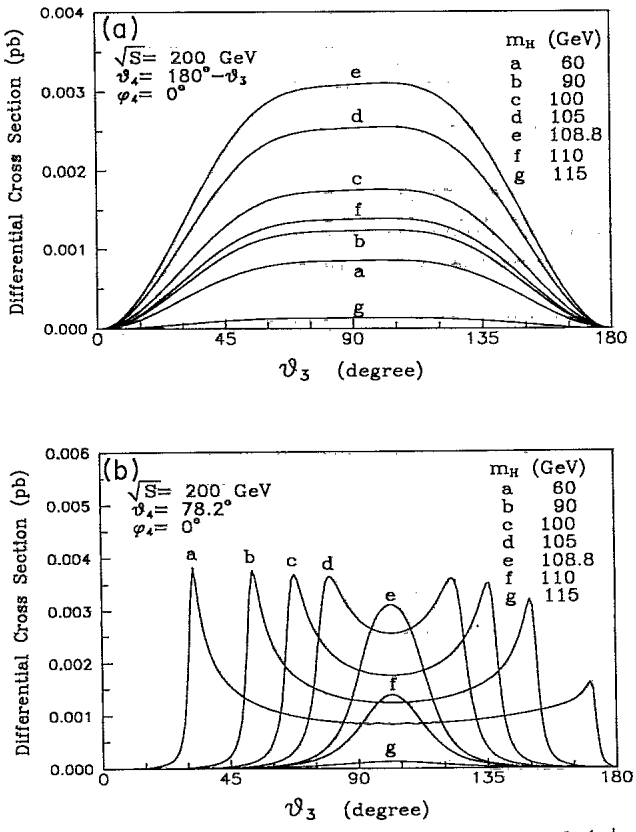

FIG. 2. Differential cross section $d\sigma(e^+e^- \to H^0\mu^+\mu^-)/d\theta_3 d\theta_4 d\phi_4$ at $\sqrt{s} = 200$ GeV shown as a function of θ_3 for (a) $(\theta_4, \phi_4) = (180° - \theta_3, 0°)$ and (b) $(\theta_4, \phi_4) = (78.2°, 0°)$. Different choices of the Higgs boson mass m_H in the range of 60–120 GeV are used for illustration.

In the c.m. frame, we may choose the kinematics

$$\begin{aligned} \mathbf{p}_1 &= -\mathbf{p}_2 = \tfrac{1}{2}\mathbf{P}, \\ \mathbf{P}\cdot\mathbf{p}_3 &= |\mathbf{P}||\mathbf{p}_3|\cos\theta_3, \\ \mathbf{P}\cdot\mathbf{p}_4 &= |\mathbf{P}||\mathbf{p}_4|\cos\theta_4, \\ \frac{\mathbf{p}_3\cdot\mathbf{p}_4}{|\mathbf{p}_3||\mathbf{p}_4|} &= \cos\theta_3\cos\theta_4 - \sin\theta_3\sin\theta_4\cos\phi_4 \\ &\equiv \Phi(\theta_3,\theta_4,\phi_4)+1, \end{aligned} \tag{5}$$

$|\mathbf{P}| \simeq \sqrt{s}$ (total c.m. energy).

We may choose the coordinate system such that the beam direction defines the z axis while μ^+ emits in the direction of $(\theta_3, 180°)$ (i.e., $\phi_3 = 180°$). Thus μ^- emits in the direction specified by (θ_4, ϕ_4).

Neglecting terms in m_e^2, we obtain the c.m. differential cross section as follows:

$$\begin{aligned} \frac{d\sigma(e^+e^-\to H\mu^+\mu^-)}{d\theta_3 d\theta_4 d\phi_4} &= \frac{1}{1024(2\pi)^4}\frac{e^6}{(\sin\theta_W\cos\theta_W)^6}\sin\theta_3\sin\theta_4 \\ &\times\int_0^{(s-m_H^2)/2\sqrt{s}} dE_3\left\{\frac{E_3E_4}{M_Z^6}\frac{1}{\sqrt{s}+E_3\Phi(\theta_3,\theta_4,\phi_4)}\right. \\ &\times\frac{1}{[1+2M_Z^{-2}E_3E_4\Phi(\theta_3,\theta_4,\phi_4)]^2+\Gamma_Z^2M_Z^{-2}}\frac{1}{(1-M_Z^{-2}s)^2+M_Z^{-2}\Gamma_Z^2} \\ &\left.\times[c_1E_3E_4(1-\cos\theta_3\cos\theta_4)+c_3m_\mu^2+c_5E_3E_4(\cos\theta_4-\cos\theta_3)]\right\}, \end{aligned} \tag{6}$$

with, as a result of energy-momentum conservation,

$$E_4 = \frac{s-2\sqrt{s}E_3-m_H^2}{2[\sqrt{s}+E_3\Phi(\theta_3,\theta_4,\phi_4)]}. \tag{7}$$

Note that, for $m_H \gg m_\mu$, the integration limits are determined simply by $E_3 = 0$ or $E_4 = 0$; that is, the heavy particle can balance the three-momentum without carrying away much of the energy.

In Figs. 2(a) and 2(b), the differential cross section $d\sigma(e^+e^-\to H^0\mu^+\mu^-)/d\theta_3 d\theta_4 d\phi_4$ at $\sqrt{s} = 200$ GeV is shown as a function of θ_3 for (a) $(\theta_4,\phi_4) = (180°-\theta_3, 0°)$ and (b) $(\theta_4,\phi_4) = (78.2°, 0°)$. Different choices of the Higgs particle mass in the range of 60–120 GeV are used for illustration.

Note that, in plotting Fig. 2(a), we have chosen $\theta_4 = 180° - \theta_3$ and $\phi_4 = 0$ on the basis that the differential cross section is the largest for back-to-back $\mu^+\mu^-$ pairs. The differential cross section at $\sqrt{s} = 200$ GeV has the maximum of 8.6×10^{-4} pb for $m_H = 60$ GeV, 3.1×10^{-3} pb for $m_H = 108.8$ GeV, and 1.3×10^{-4} pb for $m_H = 115$ GeV, respectively.

We also note that the initial increase with m_H in the differential cross section, which can be understood as due to how far the position determined by the given kinematics is away from the pole, is somewhat misleading since the integrated total cross section decreases quickly with m_H. The maximum appears at $\theta_3 = 107.77°$, rather than 90°, due to charge asymmetry produced by the parity-violating nature of the coupling of the leptons to the Z^0 boson. The position of the maximum, say, $\theta_3 = \theta_3^m$ in a plot such as Fig. 2(a), is in fact related to the electroweak mixing parameter $\sin^2\theta_W$ as follows:

$$\begin{aligned} &(1-4\sin^2\theta_W)^2 \\ &= -\frac{1}{\cos^3\theta_3^m}\{(\cos^3\theta_3^m - 3\cos^2\theta_3^m + 1) \\ &\quad -(-6\cos^5\theta_3^m + 9\cos^4\theta_3^m + 2\cos^3\theta_3^m \\ &\quad -6\cos^2\theta_3^m + 1)^{1/2}\}. \end{aligned} \tag{8}$$

Note that $\theta_3^m > 90°$ or $\cos\theta_3^m < 0$.

Figure 2(b) indicates that, if we fix the position of the counter to detect μ^- by choosing (θ_4,ϕ_4), the cross section as a function of θ_3 is narrowly peaked at the opposite direction, ensuring again the back-to-back kinematics for the maximum cross sections. For the sake of illustration, we have taken $\theta_4 = 78.2°$ and $\phi_4 = 0°$ (where $\theta_3 \approx \theta_3^m$) in obtaining Fig. 2(b).

Returning to our discussion concerning charge asymmetry, we may define the charge asymmetry explicitly as follows:

$$\mathcal{A} \equiv \frac{d\sigma(\mu^+\mu^-)/d\theta_3 d\theta_4 - d\sigma(\mu^-\mu^+)/d\theta_3 d\theta_4}{d\sigma(\mu^+\mu^-)/d\theta_3 d\theta_4 + d\sigma(\mu^-\mu^+)/d\theta_3 d\theta_4}. \tag{9}$$

In Fig. 3, the charge asymmetry is shown as a function of θ_3 for $\theta_4 = 90°$ and $180° - \theta_3$, respectively. Note that charge asymmetry arises from the parity-violating nature of the interactions induced by Z^0. Note also that, to a sufficiently good approximation, the result shown in Fig. 3 is in fact independent of $\sqrt{s}$, m_H, and ϕ_4. This

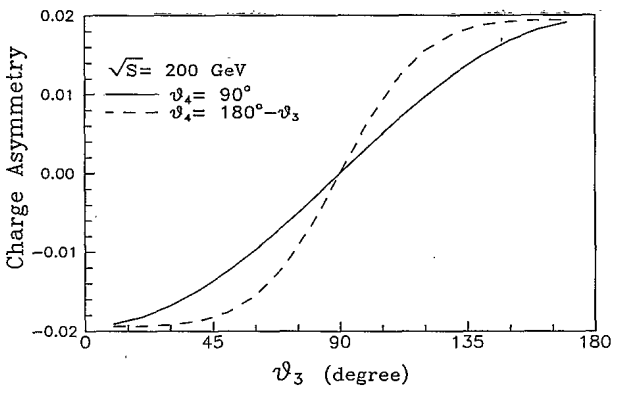

FIG. 3. Charge asymmetry as defined by Eq. (9) in the text shown as a function of θ_3 for $\theta_4 = 90°$, $180° - \theta_3$, respectively.

can be seen from Eq. (6) since, by dropping the term in m_μ, we have

$$\mathcal{A} = \frac{c_5}{c_1}\frac{\cos\theta_4 - \cos\theta_3}{1-\cos\theta_3\cos\theta_4} = 0.0194\frac{\cos\theta_4 - \cos\theta_3}{1-\cos\theta_3\cos\theta_4}, \quad (10)$$

which is independent of $\sqrt{s}$, m_H, and ϕ_4. Using Eqs. (4) and (10), one may easily obtain the relation between the observed charge asymmetry and the electroweak mixing parameter $\sin^2\theta_W$.

We may integrate out certain angles to obtain the partially integrated differential cross sections

$$\frac{d\sigma(e^+e^- \to H\mu^+\mu^-)}{d\theta_3} \equiv \int d\theta_4 d\phi_4 \frac{d\sigma(e^+e^- \to H\mu^+\mu^-)}{d\theta_3 d\theta_4 d\phi_4}, \quad (11a)$$

$$\frac{d\sigma(e^+e^- \to H\mu^+\mu^-)}{d\theta_4} \equiv \int d\theta_3 d\phi_4 \frac{d\sigma(e^+e^- \to H\mu^+\mu^-)}{d\theta_3 d\theta_4 d\phi_4}, \quad (11b)$$

$$\frac{d\sigma(e^+e^- \to H\mu^+\mu^-)}{d\phi_4} \equiv \int d\theta_3 d\theta_4 \frac{d\sigma(e^+e^- \to H\mu^+\mu^-)}{d\theta_3 d\theta_4 d\phi_4}. \quad (11c)$$

In Fig. 4, the partially integrated differential cross section $d\sigma(e^+e^- \to H^0\mu^+\mu^-)/d\theta_3$ at $\sqrt{s} = 200$ GeV is shown as a function of θ_3 for different choices of the Higgs boson mass in the range of 60–120 GeV. Here it is seen that, unlike Fig. 2(a), the decrease with the Higgs boson mass m_H is clearly at work.

In Fig. 5, the partially integrated differential cross section $d\sigma(e^+e^- \to H^0\mu^+\mu^-)/d\theta_4$ at $\sqrt{s} = 200$ GeV is shown as a function of θ_4 for different choices of the Higgs boson mass in the range of 60–120 GeV.

In Fig. 6, the partially integrated differential cross section $d\sigma(e^+e^- \to H^0\mu^+\mu^-)/d\phi_4$ at $\sqrt{s} = 200$ GeV is shown as a function of ϕ_4 for different choices of the Higgs boson mass in the range of 60–120 GeV. It is of some interest to note that the maximum does not occur at $\phi_4 = 0$, although it gradually moves over to $\phi_4 = 0$ as m_H increases.

Finally, we obtain the total cross section as defined by

$$\sigma(e^+e^- \to H\mu^+\mu^-) \equiv \int d\theta_3 \frac{d\sigma(e^+e^- \to H\mu^+\mu^-)}{d\theta_3}. \quad (12)$$

The formula for the total cross section may be obtained in the following alternative manner. Starting from Eqs. (2) and (4), we may use the momentum-conservation δ function to integrate out d^3p_4 and then use

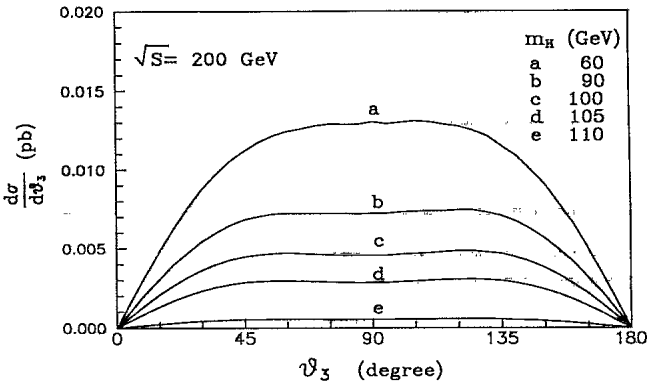

FIG. 4. Partially integrated differential cross section $d\sigma(e^+e^- \to H^0\mu^+\mu^-)/d\theta_3$ at $\sqrt{s} = 200$ GeV shown as a function of θ_3 for different choices of the Higgs boson mass in the range of 60–120 GeV.

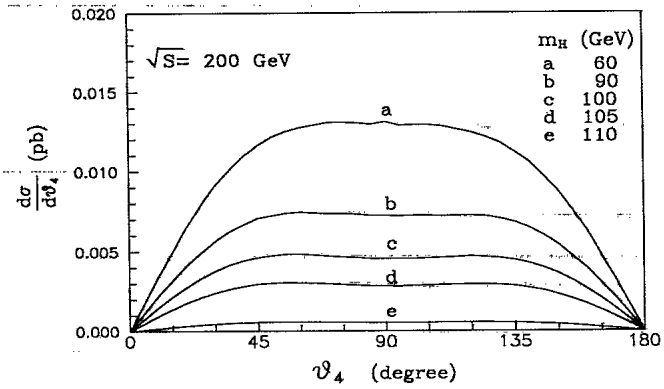

FIG. 5. Partially integrated differential cross section $d\sigma(e^+e^- \to H^0\mu^+\mu^-)/d\theta_4$ at $\sqrt{s} = 200$ GeV shown as a function of θ_4 for different choices of the Higgs boson mass in the range of 60–120 GeV.

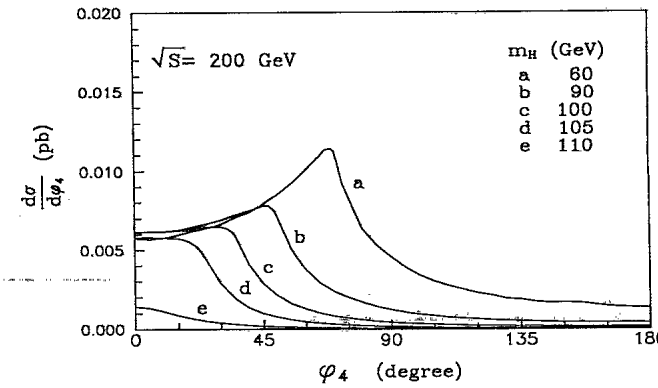

FIG. 6. Partially integrated differential cross section $d\sigma(e^+e^- \to H^0\mu^+\mu^-)/d\phi_4$ at $\sqrt{s} = 200$ GeV shown as a function of ϕ_4 for different choices of the Higgs boson mass in the range of 60–120 GeV.

$$p_4\cdot p_2 p_3\cdot p_1 + p_4\cdot p_1 p_3\cdot p_2 = \frac{s}{2}E_3\{\sqrt{s} - E_3\sin^2\theta_3 - E_H + p_H\cos\theta_3\cos\theta_H\}, \tag{13a}$$

$$p_4\cdot p_2 p_3\cdot p_1 - p_4\cdot p_1 p_3\cdot p_2 = -\frac{s}{2}E_3\{(\sqrt{s} - E_H)\cos\theta_3 + p_H\cos\theta_H\}, \tag{13b}$$

$$\delta(E_3 + E_4 + E_5 - \sqrt{s}) = \delta(\cos\theta_{53} - z_0)\frac{E_4}{E_3 p_H}, \tag{13c}$$

$$\sqrt{s} - E_H + p_H\cos\theta_{53} = \frac{s + m_H^2 - 2\sqrt{s}E_H}{2E_3}. \tag{13d}$$

Here and in what follows, we use θ_H, E_H, and p_H interchangeably with θ_5, E_5, and p_5. The interesting point here is that, instead of $d\Omega_3 d\Omega_5$, we may write $d\Omega_3 d\Omega_{53}$ with Ω_{53} the solid angle of the Higgs particle with respect to μ^+ and then use Eqs. (13a) and (13b) to carry out the integrations over $d\Omega_{53}$. The result is independent of ϕ_3, and so the integration over $d\phi_3$ just gives 2π:

$$\begin{aligned}\frac{d\sigma(e^+e^-\to H\mu^+\mu^-)}{dE_3 d\theta_3 dE_H} &= \sin\theta_3\frac{1}{2}\frac{1}{(2\pi)^3}\frac{1}{1024}\frac{e^6}{(\sin\theta_W\cos\theta_W)^6}\frac{4}{M_Z^6 s}\\ &\times\frac{1}{[1 - M_Z^{-2}(s + m_H^2 - 2\sqrt{s}E_H)]^2 + \Gamma_Z^2 M_Z^{-2}}\,\frac{1}{(1 - M_Z^{-2}s)^2 + M_Z^{-2}\Gamma_Z^2}\\ &\times\frac{s}{2}E_3\left\{c_1\left((\sqrt{s} - E_H - E_3)\sin^2\theta_3 + \frac{s + m_H^2 - 2\sqrt{s}E_H}{2E_3}\cos^2\theta_3\right)\right.\\ &\left. - c_5\frac{s + m_H^2 - 2\sqrt{s}E_H}{2E_3}\cos\theta_3\right\}.\end{aligned} \tag{14}$$

Note that Eq. (14) allows us to define a partially integrated charge asymmetry by comparing cross sections at θ_3 and $-\theta_3$.

The integrations over θ_3 [between 0° and 180°] and E_3 [between $\frac{1}{2}(\sqrt{s} - E_H - p_H)$ and $\frac{1}{2}(\sqrt{s} - E_H + p_H)$] are straightforward. This yields, using $e^2/(8M_Z^2\sin^2\theta_W\cos^2\theta_W) = G_F/\sqrt{2}$ and $c_1 = 64(Q_{eL}^2 + Q_{eR}^2)(Q_{\mu L}^2 + Q_{\mu R}^2)$ (in the notation of Glashow and Jenkins),

$$\begin{aligned}\frac{d\sigma(e^+e^-\to H\mu^+\mu^-)}{dE_H} &= \frac{G_F^3}{3\sqrt{2}\pi^3}(Q_{eL}^2 + Q_{eR}^2)(Q_{\mu L}^2 + Q_{\mu R}^2)\\ &\times\frac{1}{[1 - M_Z^{-2}(s + m_H^2 - 2\sqrt{s}E_H)]^2 + \Gamma_Z^2 M_Z^{-2}}\,\frac{1}{(1 - M_Z^{-2}s)^2 + M_Z^{-2}\Gamma_Z^2}\\ &\times p_H\left(s + \frac{E_H^2}{3} + \frac{2}{3}m_H^2 - 2\sqrt{s}E_H\right),\end{aligned} \tag{15}$$

which agrees with the master formula obtained by Glashow and Jenkins [12]. As a consistency check, we have chosen to integrate Eq. (6) directly and obtained numerical results identical to what Eq. (15) yields.

In Fig. 7, the total cross section $\sigma(e^+e^-\to H^0\mu^+\mu^-)$ is shown as a function of the e^+e^- center-of-mass energy $\sqrt{s}$ for different choices of the Higgs boson mass in the range of 60–200 GeV. As noted previously by Glashow and Jenkins [12], the structure of having two clearly separated peaks is very visible for m_H in the range between about 10 GeV and somewhat below the Z^0 mass and the first peak disappears for $m_H > m_Z$ because a real Z^0 can no longer decay into a Higgs particle and a $\mu^+\mu^-$ pair. Note that the result shown in Fig. 7 is very much similar to what Glashow and Jenkins [12] obtained, except that we have adopted a Higgs particle in a higher mass range (as most of their choices of the Higgs boson mass have now been ruled out by the recent LEP experiments).

In Fig. 8, the total cross section $\sigma(e^+e^-\to H^0\mu^+\mu^-)$ is shown as a function of the Higgs boson mass for the various e^+e^- center-of-mass energies.

It may be worth pointing out the important fact that the width of the Z^0, which has been considerably sharpened to a value of 2.487±0.010 GeV by the recent LEP experiments, dictates very much the magnitude of the

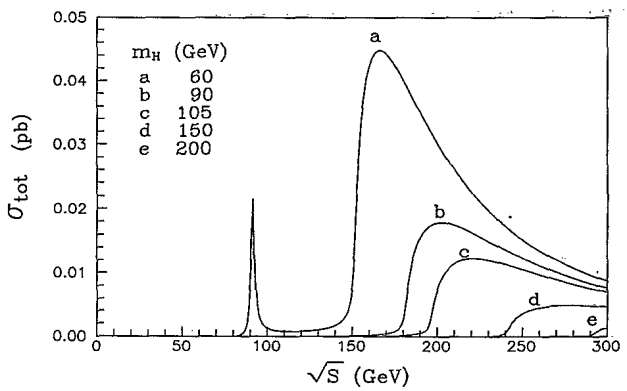

FIG. 7. Total cross section $\sigma(e^+e^-\to H^0\mu^+\mu^-)$ shown as a function of the e^+e^- center-of-mass energy $\sqrt{s}$ for different choices of the Higgs boson mass in the range of 60–200 GeV.

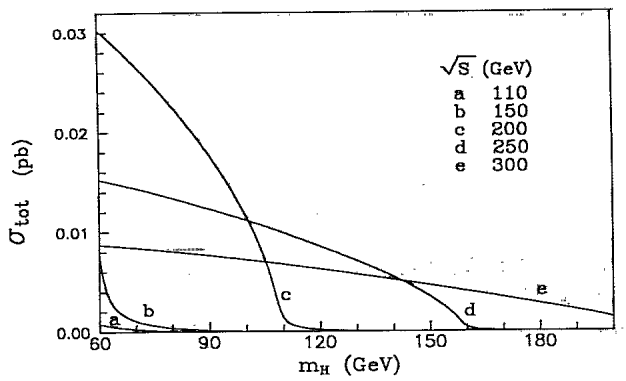

FIG. 8. Total cross section $\sigma(e^+e^- \to H^0\mu^+\mu^-)$ shown as a function of the Higgs boson mass m_H for the various e^+e^- center-of-mass energies.

cross sections [according to Eqs. (6) and (15)]. A precise value of Γ_Z has made it possible for making reliable predictions (much more precise than those given earlier [12,13]) on the production cross sections of the standard Higgs particle.

In closing the presentation of our sample numerical results, it is of critical importance to note that, in obtaining results reported in Figs. 2–6, we did not attempt to choose $\sqrt{s}$ such that the integrated cross section will be at its maximum for a given Higgs boson mass, which occurs at M_Z (if $m_H \leq M_Z$) and $M_Z + m_H$. By being able to sit on top of one of the peak values (which is the case for existing Higgs particle searches [4]), the results presented in Figs. 2–6 are similar except that the scale should be increased according to what has been shown in Fig. 7.

To close this section, we note that, for cross sections of the order of 10^{-2} pb (which is typical according to our numerical results), the integrated luminosity needed to see just one event is 100 pb^{-1}, a number sensible compared to the expected total luminosity per year per detector of about 30 pb^{-1} at LEP during the next couple of years. As a benchmark, the integrated luminosity accumulated so far from the four LEP detectors since 1989 is about 300 pb^{-1}. We see from Fig. 8 that LEP II may allow us to search for the standard Higgs boson with a mass up to about 100 GeV.

III. SUMMARY

In this paper, we have investigated Higgs boson production via the Bjorken process, $e^+e^- \to H^0\mu^+\mu^-$, for a center-of-mass energy $\sqrt{s}$ of up to 200 GeV in the standard Glashow-Salam-Weinberg electroweak theory for a Higgs boson mass ranging from 60 to 120 GeV The high mass Higgs boson mass range has been chosen owing to the latest experimental situation [4] concerning Higgs particle searches. In addition, we have focused on physical quantities which have not been emphasized so far, including the differential cross sections in the various μ^+ (or μ^-) scattering angles (with the remaining angles integrated out completely) and the anticipated charge asymmetry. Numerical results on these quantities, in addition to the total production cross section, are described in some detail. The results described in this paper are complementary to those reported by Glashow and Jenkins [12] as well as by Terazawa and Biyajima [13] (the latter require simultaneous precision measurements of both μ^+ and μ^-).

ACKNOWLEDGMENTS

This work was supported in part by grants from the National Science Council of Republic of China under Grant No. NSC83-0208-M0020-025Y. One of us (W-Y.P.H.) wishes to also acknowledge the Alexander von Humboldt Foundation for support during a visit to Jülich, during which the initial version of this manuscript was prepared.

[1] S. Weinberg, Phys. Rev. Lett. **19**, 1264 (1967); A. Salam, in *Elementary Particle Theory*, edited by N. Svartholm (Almquist and Wiksells, Stockholm, 1969), p. 367; S. L. Glashow, J. Iliopoulos, and L. Maiani, Phys. Rev. D **2**, 1285 (1970).

[2] Particle Data Group, K. Hikasa *et al.*, Phys. Rev. D **45**, S1 (1992).

[3] S. Weinberg, Phys. Rev. Lett. **36**, 294 (1976); M. Veltman, Ann. Phys. (N.Y.) B **8**, 475 (1977); B. W. Lee, C. Quigg, and H. B. Thacker, Phys. Rev. D **16**, 1519 (1977); S. Raby, G. B. West, and C. M. Hoffman, *ibid.* **39**, 828 (1989).

[4] See "Gauge and Higgs Boson Full Listings" in Ref. [2] for detailed experimental references.

[5] F. Wilczek, Phys. Rev. Lett. **39**, 1304 (1977).

[6] R. N. Cahn, M. S. Chanowitz, and N. Fleishon, Phys. Lett. **82B**, 113 (1979).

[7] J. Ellis, M. K. Gaillard, and D. V. Nanopoulos, Nucl. Phys. **B106**, 292 (1976).

[8] S. L. Glashow, D. Nanopoulos, and A. Yildiz, Phys. Rev. D **18**, 1724 (1978).

[9] D. Atwood, A. P. Contogouris, and K. Takeuchi, Phys. Rev. D **38**, 3437 (1988).

[10] P. R. Burchat, D. L. Burke, and A. Petersen, Phys. Rev. D **38**, 2735 (1988).

[11] J. D. Bjorken, "Weak Interaction Theory and Neutral Currents," in Proceedings of the SLAC Summer Institute 1976, SLAC Report No. 198 (unpublished); B. L. Ioffe and V. A. Khoze, Sov. J. Part. Nucl. **9**, 50 (1978).

[12] S. L. Glashow and E. E. Jenkins, Phys. Lett. B **206**, 522 (1988).

[13] T. Morioka, M. Biyajima, and O. Terazawa, Prog. Theor. Phys. **76**, 1089 (1986); O. Terazawa and M. Biyajima, Phys. Rev. D **39**, 736 (1989).